Improving Low-Contrast Images Using Frequency and Fuzzy Transformations

Lyudmila Akhmetshina[a], Artyom Yegorov[a] and Stanislav Mitrofanov[a]

[a] *Dnieper National University Named by Oles Honchar, Gagarin Avenue, house 72, Dnieper, 49010, Ukraine*

Abstract

The informational capabilities of a method for processing grayscale images aimed at improving contrast and increasing object detail to increase the accuracy of diagnosis based on them are presented. The proposed adaptive composite algorithm is based on multi-stage processing, which includes the use of two-dimensional frequency Fourier transformation and the method of fuzzy intensification in the spatial domain, and makes several transitions between different feature spaces. The application of the Fourier transform involves the correction of its coefficients and the reconstruction of the image by inverse transformation. Only arguments of complex coefficients can be adjusted. The impact of the frequency transformation parameters on the detail of the resulting image is analyzed. The method of fuzzy intensification is used as a refinement for the second stage of frequency transformation. The results of processing are presented on the example of real X-ray images.

Keywords 1

low-contrast images, two-dimensional Fourier transform, fuzzy intensification operator.

1. Introduction

The number of areas in which the raw data comes in the form of images is constantly growing. These include surveillance, monitoring, polygraphy, medicine and many other areas. The role of computer vision systems, which implement methods of improving the quality of digital images for further visual or automatic analysis in order to make accurate decisions based on them, is growing [1].

For example, medical images, which are an integral part of the diagnosis of various diseases, usually have low resolution (in the spatial and spectral domain), high level of noise, weak contrast, geometric deformations, as well as various types of uncertainty and inaccuracy. In addition, the insufficient sensitivity of the human eye perceives, according to Weber's law, only a 2% difference in brightness (the gray level of a standard monitor is approximately 0.04%), and this value significantly depends on the surrounding background, which reduces the ability to detect low-intensity objects of interest based on visual analysis [2].

It is important to note that appropriately assessing the quality of the image is quite a difficult task, since the characteristics of the image as a whole and in local areas (areas of interest) can differ significantly. This makes it difficult to automatically calculate the quantitative value of the overall quality assessment of both the raw data and the processing result. In practice, expert evaluations are usually used to determine the quality of images.

The Sixth International Workshop on Computer Modeling and Intelligent Systems (CMIS-2023), May 3, 2023, Zaporizhzhia, Ukraine

EMAIL: akhmlu1@gmail.com (L. Akhmetshina); for___students@ukr.net (A. Yegorov); stas.mitrofanov1337@gmail.com (S. Mitrofanov)

ORCID: 0000-0002-5802-0907 (L. Akhmetshina); 0000-0002-7558-785X (A. Yegorov); 0009-0005-5491-7740 (S. Mitrofanov)

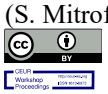

Digital processing of medical images allows to significantly improve their quality, in particular, contrast and resolution [3, 4]. Due to the huge variety of types of images, there are currently no universal methods that provide a guaranteed result of solving this problem [5].

X-ray images, which are an important diagnostic tool for many diseases, are characterized by low intensity, uneven background, high level of noise, weak contrast, and poorly defined boundaries of structures, and are particularly difficult to analyze and choose an effective processing method [6].

2. Review of Literature

Approaches to the improvement of digital images are usually divided into two categories: processing methods in the spatial and frequency domains [7]. The concept of "spatial transformations" combines approaches that are based on the direct change of brightness values of pixels of raster images [8-10].

Frequency methods, in particular, change not the image, but the form of its representation, converting the output signal into its components of different frequencies and amplitudes. In this form, it is much easier to perform filtering or amplification of individual components of the signal, to highlight important parameters whose detection by other methods is less effective or impossible [11]. Such algorithms are quite effective from the perspective of denoising signal, do not require a priori information, which is often absent in practice. This mathematical tool is widely used in medical imaging in the formation of CT, MRI and ultrasound images of human anatomy [12].

These medical images, besides the shortcomings caused by weak lighting exposure, noise, low contrast, etc., include uncertainty and fuzziness, which complicates the extraction of necessary information. Thus, the task of improving their quality is an essential task for carrying out a proper diagnosis. In [13], various fuzzy logic methods are considered for this purpose, which, like the frequency domain, allows obtaining an additional feature space for analysis.

Since the 1980s, fuzzy set theory [14] has been used for image processing, which has the ability to model the problems associated with uncertainty and inaccuracy, which are always present in digital images. Their presence is determined both by the features of the physical processes of image formation systems and by the stage of creating a digital image [15].

The main difference between fuzzy methods and other processing methodologies is that the input data (gray levels, histograms, features, etc.) are transformed into a fuzzy domain. An $M \times N$ image G with L L gray levels can be represented as an array of fuzzy sets with respect to the analyzed property with the value of the membership function μ_{mn}, which varies in the interval $[0,1]$ for each pixel x_{mn}:

$$G = \bigcup_{m=1}^{M} \bigcup_{n=1}^{N} \frac{\mu_{mn}}{x_{mn}}. \quad (1)$$

The transition to a fuzzy domain (fuzzification) can be interpreted as a specific type of input data encoding, which depends on both the goal and the characteristics of the output image. The use of fuzzy logic makes it possible to obtain new effective algorithms for processing digital images (fuzzy clustering, equalization, intensification, etc.) [17-19].

Based on the features and characteristics of different types of medical images, a combination of different algorithms is usually used to obtain a good processing result [18, 20, 21].

3. Problem statement

The paper is devoted to the description and experimental research of a new adaptive composite method for enhancing low-contrast images by increasing contrast and detail level, which combines frequency and fuzzy transformations and makes several transitions between different feature spaces.

4. Materials and Methods

For an image of size $M \times N$, which is described by a real two-dimensional discrete function $F(x, y)$ the discrete two-dimensional Fourier transform (2D DFT) provides the creation of a complex

two-dimensional function, which is defined in a frequency coordinate system (u,v) based on the expression:

$$F(u,v) = \frac{1}{M \cdot N} \cdot \sum_{x=0}^{M-1} \sum_{y=0}^{N-1} F(x,y) e^{i \cdot 2 \cdot \pi \cdot \left(\frac{ux}{M} + \frac{vy}{N} \right)}. \quad (2)$$

The basis functions are sinusoidal and cosinusoidal waves with increasing frequencies. $F(0,0)$ represents the constant component of the image, which corresponds to the average brightness, and $F(M-1, N-1)$ represents the highest frequency [11].

The 2D DFT is a selective Fourier transform and therefore does not contain all frequencies that make up the image, but only a set of samples that are sufficient to describe the image in the spatial domain. The number of frequencies corresponds to the number of pixels in the image and allows access to the geometric characteristics of the image in the spatial domain.

The inverse two-dimensional discrete Fourier transform (2D IDFT) is given by:

$$F(x,y) = \sum_{u=o}^{M-1} \sum_{v=0}^{N-1} F(u,v) \cdot e^{i \cdot 2 \cdot \pi \cdot \left(\frac{ux}{M} + \frac{vy}{N} \right)}. \quad (3)$$

The ranges of changes in spatial $x = 0,1,2,...,M-1$, $y = 0,1,2,...,N-1$ and frequency coordinates $u = 0,1,2,...,M-1$, $v = 0,1,2,...,N-1$ are the same.

The Fourier transform always creates an output image with a complex number value:

$$F(u,v) = R(u,v) + i \cdot I(u,v), \quad (4)$$

where $R(u,v)$ and $I(u,v)$ are real and imaginary components of $F(u,v)$.

The main method of using this transform for image analysis and transformation is by computing and visualizing the spectrum.

$$| F(u,v) | = \sqrt{R^2(u,v) + I^2(u,v)}. \quad (5)$$

It is the amplitude of the Fourier transform that contains most of the image information in the spatial domain. The higher the value of $| F(u,v) |$, the brighter the point with coordinates (u,v). The bright center of the spectrum means that the original image contains mostly homogeneous areas, without differences in brightness. Bright periphery - many local differences in brightness.

In the phase spectrum which is calculated by the formula:

$$\phi(u,v) = \arctan\left(\frac{I(u,v)}{R(u,v)} \right), \quad (6)$$

the value of each point determines the shift from the components of the image. At zero phase, all sinusoids are centered in the same place, resulting in a symmetrical image, the structure of which has no real correlation with the original image. The phase reflects to a certain extent the location of the harmonic components in a spatial domain.

The importance of phase is particularly evident in certain specific areas, such as optical metrology, materials science, adaptive optics, X-ray diffraction optics, electron microscopy, and biomedical imaging. The most interesting samples relate to phase objects with very low absorption but with a non-uniform spatial distribution of their refractive index or thickness. This leads to small variations in amplitude but significant variations in phase components. [11].

Figure 1a shows a typical X-ray image and its histogram. The weak contrast is due to the limited range of reproducible brightness. An optimally visually perceptible image has a brightness distribution close to normal and a wide dynamic range, and is interpreted as a high-contrast image when the levels are distributed close to uniform. A classical low-contrast image has a narrow histogram located near the center of the brightness range. In this case, standard methods such as histogram equalization, linear contrast enhancement, gamma correction, and gradient mapping provide good results [1, 2].

Unlike low-contrast images, the characteristics of the image shown in Figure 1a, which we call "weakly-contrasted," can be formulated as follows:

- a full (or almost full) range of gray levels with significant dark and light areas;
- a multimodal histogram;

- a smooth transition of brightness in "regions of interest" (below the threshold of visual perception) and blurred boundaries between them;
- intensity levels are changed significantly in different areas;
- anomalies are not always obvious (and may be absent) and are often compared to the level of noise;
- low signal-to-noise ratio and complex structured background;
- significantly different in quality (for the same object and recording method), depending on the conditions of formation (quality of film, equipment, recording time), making the analysis task particularly difficult.

Figure 1b shows the result of applying adaptive histogram equalization (window size 8x8 pixels, uniform transformation function for the window), while Figure 1c shows the frequency domain transformation based on the expression.

$$F'(u,v) = \left|F(u,v)\right|^{r} \cdot e^{i\cdot\phi(u,v)}, \tag{7}$$

where r is the transformation parameter (which significantly affects the result and requires tuning; the value used to obtain the image in Figure 1c was $r = 0.8$). 2D IDFT (3) is applied to the matrix $F'(u,v)$, as a result, the resulting image is formed, which is scaled to the range of $[0,1]$.

Figure 1d shows the result of processing with the fuzzy intensification operator [14]. The transition to the fuzzy domain is based on the values $I_{\max}$, I_{mid} are the maximum and average values of the input image, respectively, and the parameters $F_e = 2$ and F_d, which is calculated using the formula:

$$F_d = \frac{I_{\max} - I_{mid}}{0.5^{\frac{-1}{Fe}} - 1}, \tag{8}$$

The membership function for I_{mn} is calculated according to the formula:

$$\mu_{mn} = \left(1 + \frac{I_{\max} - I_{mn}}{F_d}\right)^{-F_e}, \tag{9}$$

and its modification is performed as follows:

$$\mu'_{mn} = \begin{cases} 2\cdot\mu^2{}_{mn}, 0 \le \mu_{mn} \le 0.5 \\ 1 - 2\cdot(1-\mu_{mn})^2, 0.5 < \mu_{mn} \le 1 \end{cases}, \tag{10}$$

The final result of processing is formed according to the following formula:

$$I_1 = I_{\max} - F_d \cdot \left(\left(\mu'_{mn}\right)^{-1/F_e} - 1\right), \tag{11}$$

The image processing results in Figure 1a indicate that, all methods provide a similar degree of improvement in contrast. However, there is no significant improvement in terms of visual analysis, such as object detection, boundary highlighting, and detailing of individual structures.

The algorithm proposed in this work can be formulated as follows:

1. 2D DFT (2) is applied to an image I, scaled to the range of $[0,1]$. This step allows to make a transition to a new feature space;
2. frequency domain transformation based on formula (7) with a coefficient of $r = 0.8$ and obtaining the matrix F_1';
3. 2D IDFT (3) is applied to matrix F_1' (returning to the original feature space), with results scaled to the range of $[0,1]$, afterwards adaptive histogram equalization is applied, which results in an image I_2. In the proposed algorithm, adaptive histogram equalization where used with window size 8x8 pixels, and uniform transformation function for the window;
4. formation of I_3, according to the formula:

$$I_3 = I_2 - \overline{I_2}, \tag{12}$$

where $\overline{I_2}$ is mean of gray levels of the I_2;

5. contrast enhancement for the image I_3, using a method based on the application of the fuzzy intensification operator, resulting in the formation of the image I_4. This step also leads to transition to a new feature space;
6. 2D DFT (2) is applied to the image I_4 and obtaining the function $F_5(u,v)$. This transformation makes transition to a new features space again;

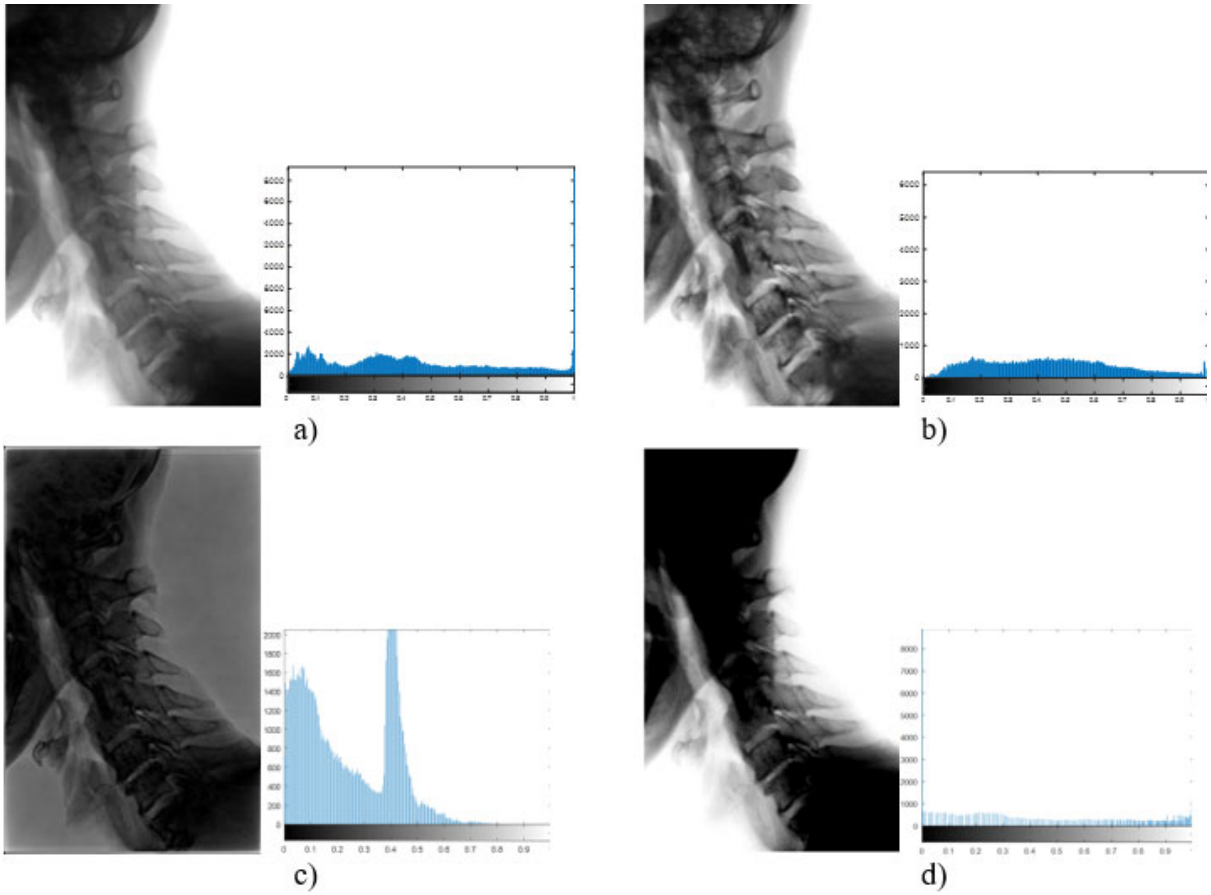

Figure 1: X-ray image processing: a – input image (459x290); results of processing by different methods: b – adaptive histogram equalization; c – Fourier transform; d – fuzzy intensification operator

7. formation of the matrix F_6 according to the following formula:

$$F_6(u,v) = \left(|F_5(u,v)|^{r_1} - |F_5(u,v)|^{r_2} \right) \cdot e^{i \cdot \phi(u,v)}. \quad (13)$$

It should be noted that the coefficients and require manual adjustment as they have a significant impact on the detailing of the result and may differ for different input images. This leads to additional time costs, so we also proposed formulas for the automatic calculation of matrices for these coefficients

$$r_1(u,v) = r_c + I_4' + \frac{I_4' + F_5'(u,v)}{2 \cdot 10 \cdot (1 + I_4')}, \quad (14)$$

$$r_2(u,v) = I_4' + \frac{F_5'(u,v)}{10}, \quad (15)$$

where $r_c = 0.5$ and I_4' is defined by the next formula:

$$I_4' = \left(0.5 + \left(\frac{I_4^{\max} + I_4^{\min}}{2} + \overline{I_4} \right) \right) / 2, \quad (16)$$

where $\overline{I_4}$ is mean of gray levels of the I_4; $I_4^{\min}$, $I_4^{\max}$ are the minimal and the maximal values of the I_4, correspondingly; $F_5'(u,v)=|F_5(u,v)|$ with following scaling of obtained matrix to the range of $[0,1]$. This method of calculation allows to control the level of detail by changing coefficient r_c in formula (14). Increasing this coefficient leads to decreasing level of detail of final image while decreasing r_c leads to increasing the level of details of resulting image;

8. 2D IDFT is applied to matrix F_6, resulting in the formation of image I_7 (returning to the original feature space), with results scaled to the range of $[0,1]$. After that, adaptive histogram equalization is used, which leads to the formation of the final result.

5. Results and Discussion

The described algorithm was used to process various X-ray images. Analysis of Figure 1a is used to calculate indicators of X-ray planimetry in patients with spinal cord and cervical spine injuries in the practice of medical and social expertise. Blurred boundaries of objects of interest and a lack of detail in their structure complicate the solution of this task.

To obtain experimental results we used Matlab 2016. Source code for described methods was written in internal Matlab language (except for standard functions like fft2, ifft2, adapthisteq, mat2gray, etc.).

Figure 2 shows the results of processing the X-ray image in Figure 1a. The study of the effect of the coefficient r shows, that its variation allows for the detection of object structures and the adjustment of their level of detail. Experimental studies have shown that using the algorithm formula (7) at step 7 also allows for an increase in contrast and resolution, but increases the contribution of noise components. Figures 2a and 2b show the results of processing the image in Figure 1a using formula (7) at step 7 for different values of r, which demonstrate an increase in the level of detail and noise reduction as it decreases.

Figure 3 shows brightness graphs of the line (its first 100 pixels) in the center of the image in Figure 1a when using formula (7) at step 7 of the proposed algorithm for values of $r=0.5$; $r=0.8$ and $r=1.2$. Based on the obtained graphs, it can be concluded that the value of parameter r in formula (7) affects the ratio of high-frequency and low-frequency components.

The use of formula (13) at step 7 of the proposed algorithm provides an adjustable increase in image detail by changing the parameters r_1 and r_2, with a decrease in the noise component. Figure 4a shows the result of the algorithm for $r_1=1.2$ and $r_2=0.7$, which show a significant improvement in visualization of the region of interest. Figure 4b presents the result of the proposed algorithm with automatic calculation of parameters r_1 and r_2 based on formulas (14), (15), which is very close to the manual selection of these parameters.

In processing many medical images, the interest is not so much in increasing the image contrast as in the redistribution of brightness levels in order to make small brightness variations more noticeable and distinguishable, which is important for visually highlighting objects of interest. In this case, the fact of their presence and location is usually unknown. In such a case, the assessment of such integral numerical characteristics as contrast or brightness level is uninformative.

In cases where the analysis area is defined (e.g., in monitoring the dynamics of disease progress), improving the visual distinguishability of the object of interest does not necessarily imply an improvement in the overall contrast level due to the increased contribution of the background component. Valid tracking of image quality changes can only be achieved by visually assessing the differences detected in the images.

One of the ways to evaluate the processing result is to analyze the brightness change graphs in the region of interest (Fig. 5). The presented brightness graphs of a portion (pixels from 40 to 140) of an arbitrary row (in this case, 220th from the top) of the input I and resulting I_7 images indicate both an increase in the dynamic range – $\Delta I_7 / \Delta I \approx 3$, and a redistribution of brightness levels in low-

contrast areas of interest. The usage of the classical method of adaptive histogram equalization (Fig. 1b) does not provide such an effect.

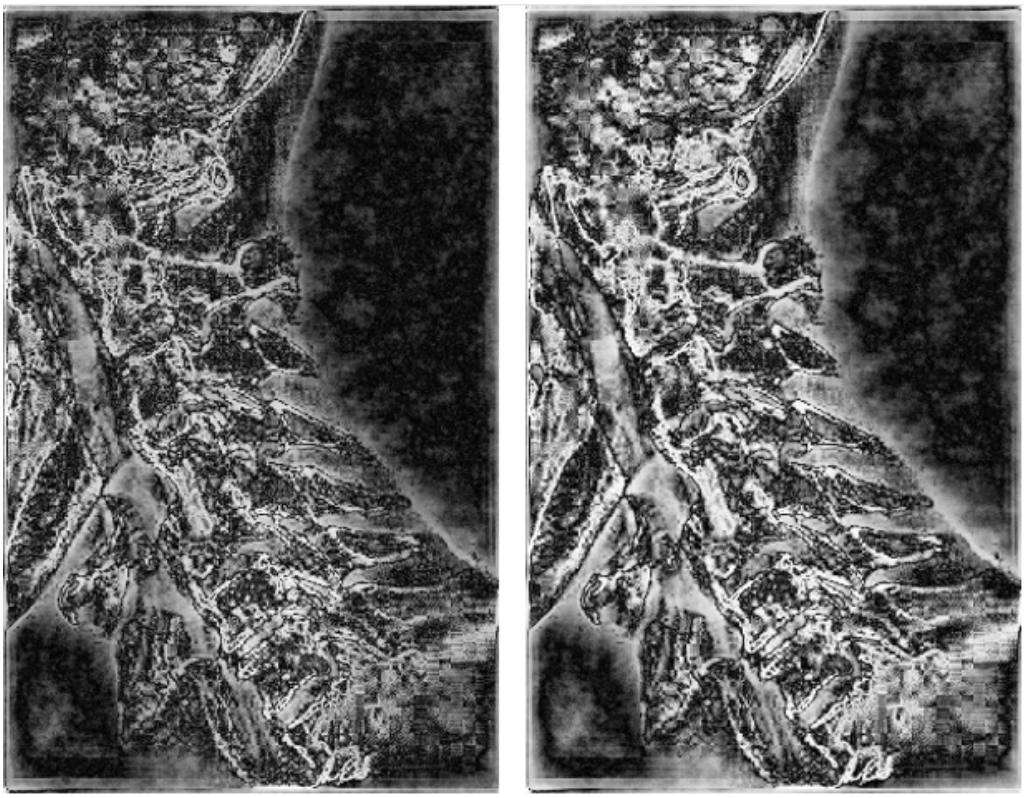

a b

Figure 2: Results of the proposed algorithm when using formula (7) at step 7 for different parameter values: a – $r = 0.7$; b – $r = 0.8$

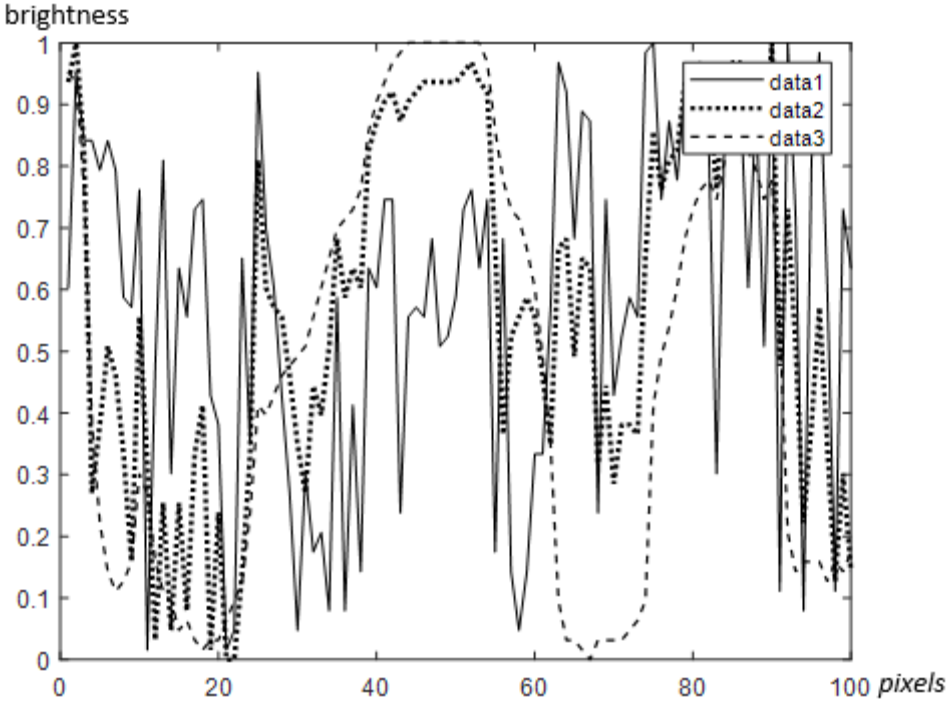

Figure 3: Changes in the brightness of a line in the center of the image for the values $r = 0.5$ (data1); $r = 0.8$ (data2); $r = 1.2$ (data3).

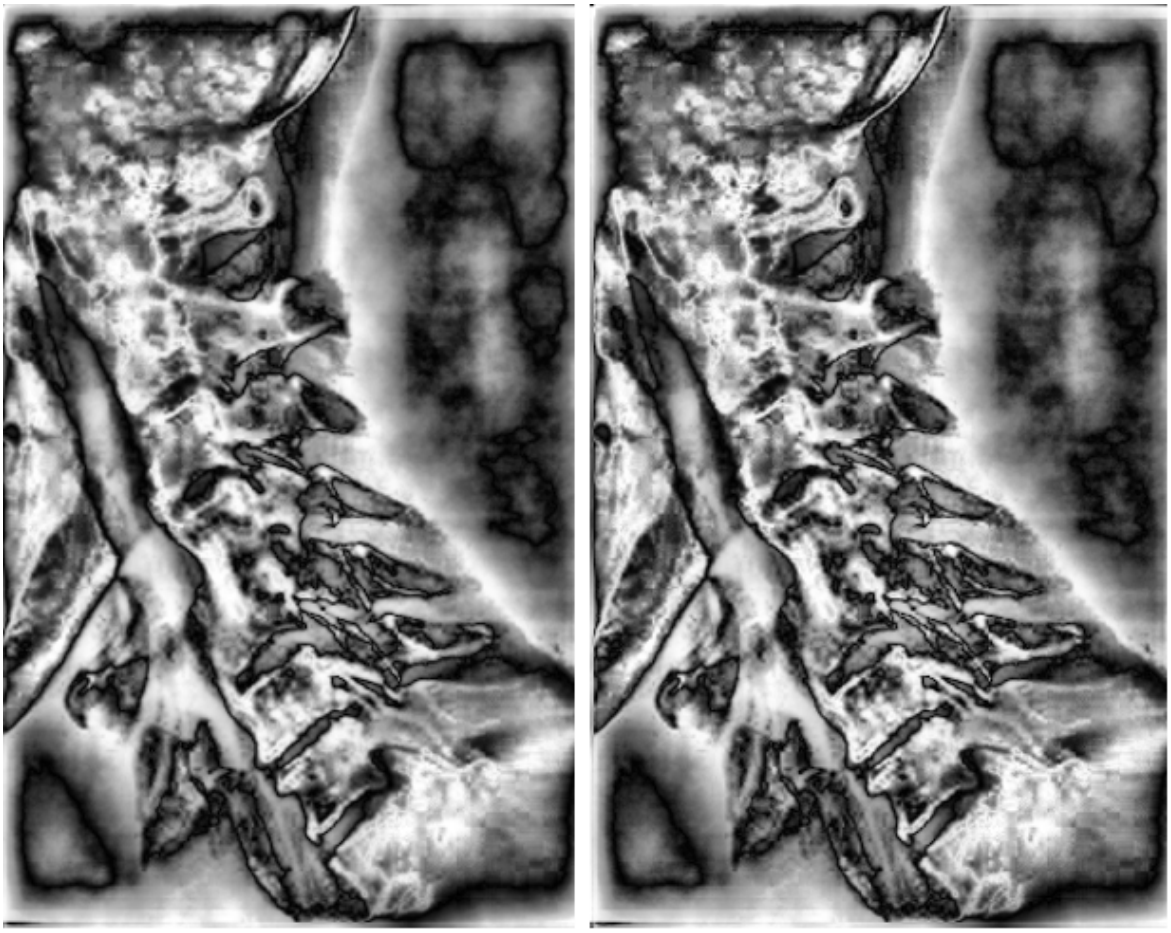

a b

Figure 4: The results of the proposed algorithm using formula (13) in step 7 for different parameter values are shown: a – $r_1 = 1.2$, $r_2 = 0.7$; b – for automatic calculation of r_1 and r_2 using formulas (14) and (15), respectively.

Figure 6a shows an X-ray image used for diagnosing inflammation (sinusitis), indicated by an arrow. The object of interest is not visible for direct visual analysis in the original image because of its location in an area of high brightness. The use of adaptive histogram equalization (Figure 6b) slightly improves the image but does not provide the necessary level of tissue structure detailing. The intensification operator (Figure 6c) worsens the original X-ray image.

The application of the proposed algorithm (Figure 6d-6f) significantly increases the image detailing in the area of low brightness values and the object of interest. In particular, the detection of the structure of the nasopharynx and oral cavity region should be noted, while the inability to visualize soft tissue is a significant drawback of X-ray research methods.

The values of r_1 and r_2 also affect the level of detail in the resulting image, as demonstrated by the comparison between Figure 6d ($r_1 = 0.95, r_2 = 0.7$) and Figure 6e ($r_1 = 1.2, r_2 = 0.7$). The improvement in the clarity of tissue structure delineation is most noticeable in the eye area. When using the automatic calculation of r_1 and r_2 based on formulas (14) and (15), the processed image (Figure 6f) is close to the best result obtained by manual selection of coefficients ($r_1 = 1.2, r_2 = 0.7$), but has a little higher level of detail due to adaptive nature of automatically calculated coefficients r_1 and r_2 . This fact confirms the effectiveness of the proposed method for automatic calculation of the method's parameters.

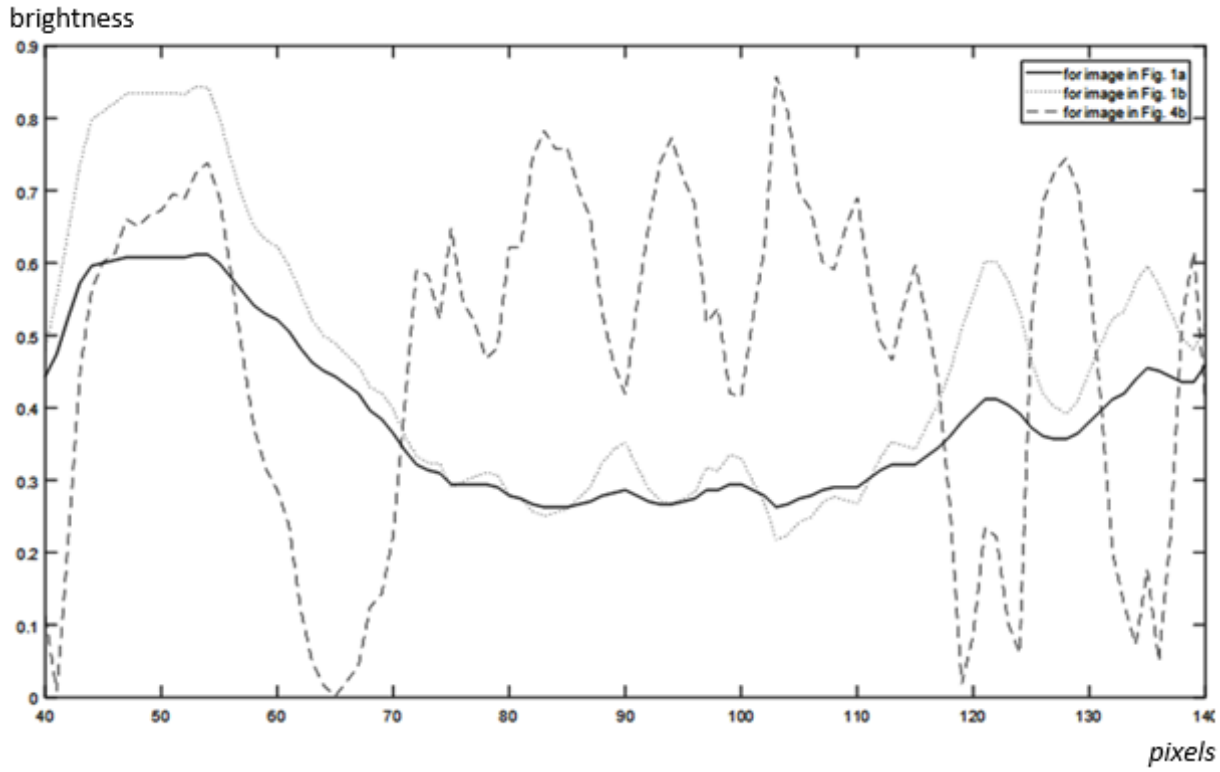

Figure 5: Changes in the brightness of a line number 220th (from the top) for its pixels from 40 to 140 for initial image (Fig. 1a) and processed images (Fig. 1b and Fig. 4b)

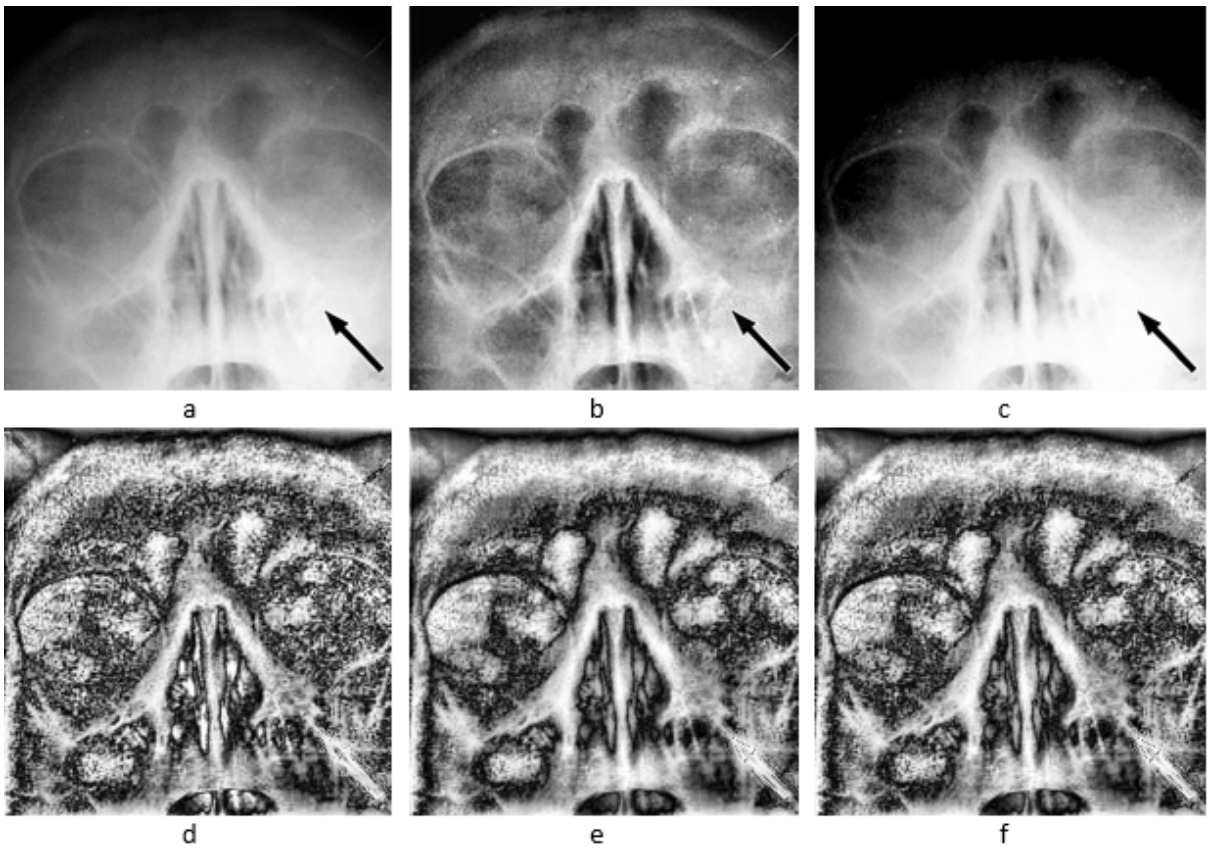

Figure 6: X-ray image of a human face: a – original image (266x272); b – adaptive histogram equalization; c – intensification operator; proposed algorithm using: d – $r_1 = 0.95$, $r_2 = 0.7$; e – $r_1 = 1.2$, $r_2 = 0.7$; f – automatic calculation of r_1, r_2 using formulas (14) and (15), respectively.

6. Conclusions

On the basis of analysis of the experimental results obtained, the following conclusions are made:

- the application of a composite adaptive algorithm for processing grayscale images, which includes the transformation of the frequency response of the 2D DFT and the method of fuzzy intensification;
- the algorithm has parameters that can be adjusted to control the level of detail in the object structure. We proposed an automatic calculation of these parameters (r_1, r_2), which reduces the time required for their selection and allows achieving a high level of detail without excessive detail effect;
- researches have shown the effectiveness of this algorithm for low-contrast images of different physical nature;
- the usage of various fuzzy transformation methods represents a promising direction for further research.

7. References

[1] D. A. Forsyth, J. Ponce, Computer Vision: A Modern Approach, 2nd. ed., Prentice Hall, 2011.

[2] R. Gonzalez, R. E. Woods, Digital Image Processing, 4th ed., Pearson, 2017.

[3] C. H. Chen, P. S. P. Wang, Handbook of pattern recognition & computer vision, 3rd ed., World Scientific Publishing Co. Pte. Ltd., 2009. doi.org/10.1142/7297.

[4] J M. Bentourkia, Fourier Analysis and Medical Image Filtering, Cambridge Scholars Publishing, 2022.

[5] S. Angenent, E. Pichon, A. Tannenbaum, Mathematical methods in medical image processing, Bulletin (New Series) of the American Mathematical Society, volume 43(3), pp. 365–396. doi: 10.1090/s0273-0979-06-01104-9.

[6] A. M. Ikhsan, A. Hussain, M. A. Zulkifley, N. Tahi, An analysis of x-ray image enhancement methods for vertebral bone segmentation Conference: 2014 IEEE 10th International Colloquium on Signal Processing & its Applications (CSPA), pp. 208-211. doi: 10.1109/CSPA.2014.6805749.

[7] W.K. Pratt, Digital Image Processing, John Wiley and Sons Inc., New York, NY, 2001.

[8] E. Pichon, A. Tannenbaum, Mathematical methods in medical image processing sigurd angenent, Bulletin (new series) of the American Mathematical Society, volume 43(3), 2006, pp. 365–396. doi: 10.1090/s0273-0979-06-01104-9.

[9] A. Mustapha, A. Hussain, S. A. Samad, A new approach for noise reduction in spine radiograph images using a non-linear contrast adjustment scheme based adaptive factor, Sci. Res. Essays, volume 6(20), 2011, pp. 4246–4258.

[10] R. Kaur, S. Guru, G. Sahib, Feature extraction and principal component analysis for lung cancer detection in ct scan images. Int. J. Adv. Res. Comput. Sci. Softw. Eng., volume 3(3), 2013, pp. 187–190.

[11] A. McAndrew, An Introduction to Digital Image Processing with Matlab, 2004.

[12] J. Luce, J. Gray, Mark A. Hoggarth, Jeffery Lin and others, Medical Image Registration Using the Fourier Transform, International Journal of Medical Physics, Clinical Engineering and Radiation Oncology, volume 3(1). doi: 10.4236/ijmpcero.2014.31008.

[13] J. Krayla, S. Kumar, U. K. Acharya and others, Comparative Analysis of Fuzzy Logic-based Image Enhancement Techniques for MRI Brain Images in: R. Asokan, D.P. Ruiz, Z.A. Baig, S. Piramuthu (Eds.) Smart Data Intelligence. Algorithms for Intelligent Systems, Springer, Singapore, 2022, pp. 447–458. doi:10.1007/978-981-19-3311-0_38.

[14] I. Bloch, Fuzzy sets for image processing and understanding, volume 281 of Fuzzy Sets and Systems, 2015, pp. 280-291. doi:10.1016/j.fss.2015.06.017.

[15] H.R. Tizhoosh, H. HauBecker, Fuzzy Image Processing: An Overview, in: B. Jähne, H. HauBecker. and P. GeiBler, (Eds.), Handbook on Computer Vision and Applications, Academic Press, Boston, volume 1, 2000, pp. 683-727.
[16] Z. Chi, H. Yan, T. Pham, Fuzzy algorithms: With Applications to Image Processing and Pattern Recognition, Singapore, New Jersey, London, Hong Kong, Word Scientific, 1998.
[17] A. Nirmala. Medical Image Denoising by Nonlocal Means with Level Set Based Fuzzy Segmentation. Indian Journal of Science and Technology, volume 10(36), 2017, pp. 1-11. doi: 10.17485/ijst/2017/v10i36/112402.
[18] A. Yegorov, L. Akhmetshina, Optimizatsiya yarkosti izobrazheniy na osnove neyro-fazzi tekhnologiy, Lambert, 2015.
[19] T. Chaira, A novel intuitionistic fuzzy C means clustering algorithm and its application to medical images, Applied Soft Computing, volume 11(2), 2011, pp. 1711–1717. doi: 10.1016/j.asoc.2010.05.005.
[20] L. Akhmetshina. A. Egorov, Low-Contrast Image Segmentation by using of the Type-2 Fuzzy Clustering Based on the Membership Function Statistical Characteristics. International Scientific Conference Lecture Notes in Computational Intelligence and Decision Making. AISC, 2020, - v. 1020. pp. 689-700.
[21] H. S. S. Ahmed, M. J. Nordin, Improving Diagnostic Viewing of Medical Images using Enhancement Algorithms, Journal of Computer Science, volume 7(12), 2011, pp. 1831-1838.